ORIGINAL RESEARCH

Attenuation of Lower-Thoracic, Lumbar, and Sacral Spinal Cord Motion: Implications for Imaging Human Spinal Cord Structure and Function

C.R. Figley
D. Yau
P.W. Stroman

BACKGROUND AND PURPOSE: Recent literature indicates that cervical and upper-thoracic spinal cord motion adversely affect both structural and functional MR imaging (fMRI; particularly diffusion tensor imaging [DTI] and spinal fMRI), ultimately reducing the reliability of these methods for both research and clinical applications. In the present study, we investigated motion of the lower-thoracic, lumbar, and sacral cord segments to evaluate the incidence of similar motion-related confounds in these regions.

MATERIALS AND METHODS: Recently developed methods, used previously for measuring cervical and upper-thoracic spinal cord motion, were employed in the present study to examine anteroposterior (A/P) and left-right (L/R) spinal cord motion in caudal regions. Segmented cinematic imaging was applied with a gradient-echo, turbo fast low-angle shot (turbo-FLASH) pulse sequence to acquire midline images of the cord at 24 cardiac phases throughout the lower-thoracic, lumbar, and sacral spinal cord regions.

RESULTS: The magnitude of A/P motion was found to be largest in rostral cord regions, whereas in caudal regions (at the level of the T4/T5 vertebrae and below), peak cord motion was uniformly small (routinely $\leq$0.10 mm). L/R motion, however, was found to be minimal throughout the thoracic, lumbar, and sacral regions.

CONCLUSION: Motion-related errors in spinal fMRI and DTI are expected to be significantly reduced throughout caudal regions of the spinal cord, thus yielding higher sensitivity and specificity compared with rostral regions. The paucity of such errors is expected to provide a means of observing the specific impact of motion (in rostral regions) and to enable the acquisition of uncorrupted DTI and fMRI data for studies of structure and function throughout lumbar and sacral regions.

By virtue of their exquisite sensitivities to changes in neuronal activity and tissue microstructure, functional MR imaging (fMRI) and diffusion tensor imaging (DTI) possess significant potential as clinical tools for investigating spinal cord injury and assessing novel therapeutic strategies.[1-8] However, both of these techniques are highly sensitive to physiologic motion, and at this juncture, the effects of spinal cord motion and CSF flow are not yet fully known, primarily because of a lack of information regarding these complex, dynamic processes. Therefore, characterization of the normal 3D kinematics of spinal cord motion is imperative to the future development of spinal fMRI and DTI methods for research and clinical applications and to better understand and diagnose spinal cord injury and disease.

Recent work has revealed a predictable, oscillatory pattern of cardiac-related spinal cord motion throughout the cervical and upper-thoracic cord regions, primarily in the rostral-caudal (R/C) and anteroposterior (A/P) directions (although there are slight intersubject variations, the cervical [C1–C8], thoracic [T1–T12], lumbar [L1–L5], and sacral [S1–S5] spinal cord segments correspond approximately with the C1–C7, T1–T10, T11–T12, and L1–L2 vertebral levels, respectively[9]).[10-15] Left-right (L/R) cord motion, on the other hand, appears to be evident only in a small subpopulation of individuals, and even in these cases, the amplitude of L/R motion is minimal.[10,15] Several independent reports have also speculated about the magnitude and character of motion-related confounds in spinal fMRI and DTI experiments, but only recently have studies been undertaken to elucidate the specific effects of spinal cord motion and the extent to which this will probably hinder spinal fMRI and DTI.[16-18] Motion-compensated analysis of spinal fMRI data has revealed that cord motion decreases both the sensitivity and selectivity to neuronal function in the cervical and upper-thoracic regions of the spinal cord.[16] Likewise, for diffusion studies of rostral spinal cord segments, cardiac-gating at different time points of the heartbeat has revealed a strong dependence between the observed diffusion properties and cardiac phase.[17,18] Thus, there is strong evidence to suggest that accurate measurements of the mean diffusivity, fractional anisotropy, and principal eigenvector (ie, the size, shape, and orientation of the diffusion tensor) are all dependent on, and confounded by, the spinal cord motion occurring throughout the cervical and upper-thoracic cord regions.

To improve spinal fMRI and DTI methods, a clear need emerges to characterize motion throughout the entire spinal cord, including the lower-thoracic, lumbar, and sacral regions.

Received February 19, 2008; accepted after revision April 8.

From the Centre for Neuroscience Studies (C.R.F., D.Y., P.W.S.), Faculty of Health Science (D.Y.), and Departments of Diagnostic Radiology (P.W.S.) and Physics (P.W.S.), Queen's University, Kingston, Ontario, Canada.

Funding for this project was provided by the International Spinal Research Trust (United Kingdom) and the Canada Research Chairs Program.

Please address correspondence to Patrick W. Stroman, Department of Diagnostic Radiology, c/o Centre for Neuroscience Studies, 228 Botterell Hall, Queen's University, Kingston, Ontario, Canada K7L 3N6; e-mail: stromanp@post.queensu.ca

DOI 10.3174/ajnr.A1154

Improved methods for cervical and upper-thoracic spinal cord fMRI and DTI have already emerged as a result of establishing the patterns of cord motion in these regions.[16-18] Thus, our objective in the present study was to extend the characterization of cardiac-related A/P and L/R spinal cord motion to the thoracic, lumbar, and sacral spinal cord regions.

Materials and Methods

Research Subjects

Data were obtained from 8 healthy volunteers (4 male and 4 female) with no history or evidence of spinal cord/vertebral injury or dysmorphology. Subject age, weight, and height ranged from 21 to 26 years (mean ± SD, 24 ± 1 years), 54 to 91 kg (mean ± SD, 67 ± 14 kg), and 1.55 to 1.83 m (mean ± SD, 1.71 ± 0.11 m) respectively. All of the participants provided informed consent before enrollment in the study, which had been approved by the institutional human research ethics board.

Study Design

All of the experiments were performed in a 3T whole-body MR imaging system (Magnetom Trio; Siemens, Erlangen, Germany), with subjects lying supine. Using a bore-mounted laser guide, subjects were carefully positioned on the scanner bed to align their shoulders and hips and to center the yaw and roll of their heads. Before scanning, a pulse oximeter was also placed on the index finger to enable segmented image acquisition and peripheral pulse recording throughout each experiment. Initial 3-plane localizer images were then acquired to provide a 3D position reference for subsequent slice alignment within each subject. All of the radio-frequency pulses were transmitted with a body coil and, for the lower-thoracic, lumbar, and sacral regions of the cord, the lower elements of a spine phased-array coil were used as receivers. Alternatively, when imaging lower-cervical and upper-thoracic spinal cord regions, signal intensity was received by a posterior neck coil and the upper elements of a spine phased-array coil.

Following the acquisition of localizer images, cardiac-gated, gradient-echo, turbo fast low-angle shot (turbo-FLASH) pulse sequences were used to study cardiac-related spinal cord motion, as reported previously.[15] In this manner, cinematic (CINE) images of the spinal cord were acquired continuously with the following parameters: TE, 2.03 ms; TR, 44.66 ms; flip, 60°; NEX, 4. Using the peripheral pulse waveform (from the pulse oximeter), image data were retrospectively gated over the course of many heartbeats to reconstruct images of the spinal cord at 24 phases throughout the cardiac cycle. Thus, cord motion data in this study, acquired from sacral, lumbar, and thoracic regions, were obtained with the same pulse sequences and imaging parameters used previously in studies of cardiac-related cervical and upper-thoracic spinal cord motion.[15] These methods have already been shown to accurately reflect spinal cord motion with an estimated error of ±0.10 mm (A/P or L/R) over a large R/C range.[15]

For every subject, A/P spinal cord motion was measured. To examine sacral, lumbar, and lower-thoracic cord motion, turbo-FLASH data were acquired from a single, 3-mm-thick, midsagittal section (200 × 200 mm^2 FOV), with its inferior margin positioned slightly below the level of the conus medullaris (ie, the caudal end of the spinal cord). The midsagittal section was then repositioned rostrally, with the inferior margin overlapping one vertebral level with the previous section position (Fig 1), so as to span the lower-thoracic to upper-thoracic or (depending on spinal cord length and curvature) lower-cervical spinal cord segments.

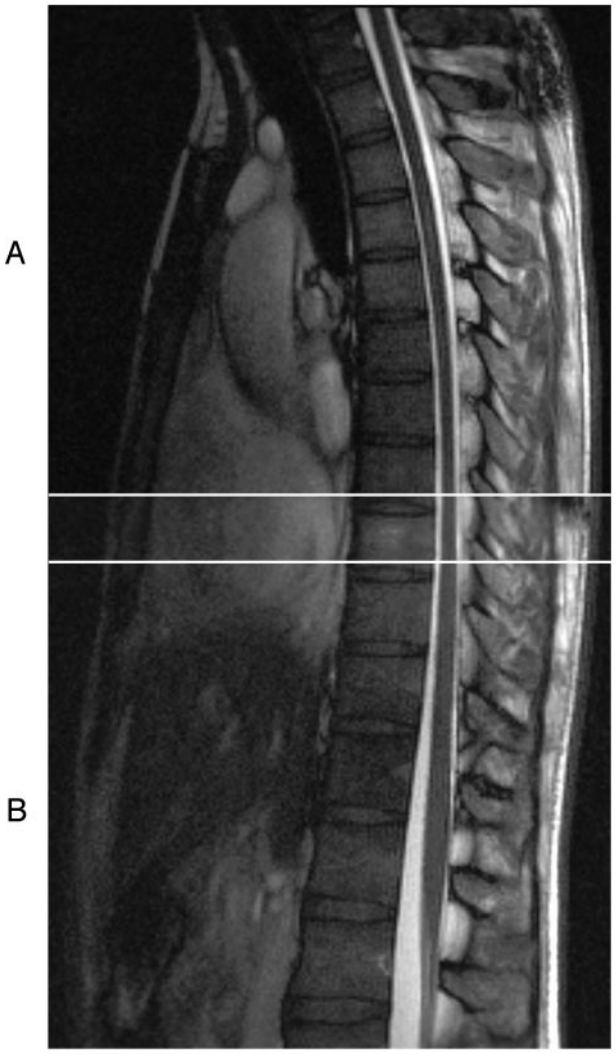

Fig 1. To characterize A/P spinal cord motion, midsagittal CINE images were acquired at 24 phases of the cardiac cycle. To span the length of the cord, 2 sets of overlapping data were acquired. *A*, Spanning the lower-cervical and upper-thoracic vertebral levels. *B*, Spanning the lower-thoracic and upper-lumbar vertebral levels (below the level of the conus medullaris). These sections were positioned such that there was approximately one vertebral level of overlap (denoted by the 2 horizontal white lines) between the rostral and caudal datasets, thus enabling uninterrupted characterization of motion along the cord.

The procedure for measuring L/R spinal cord motion was similar to that used for characterizing A/P motion, as described above. In this case, however, the image data were acquired from a single, 3-mm-thick, midcoronal section, once again having a 200 × 200 mm^2 FOV with the inferior margin situated slightly below the level of the conus medullaris. As a result of cross-subject variation in A/P spinal cord curvature, the length of cord spanned by the midcoronal section was variable across subjects. Therefore, the position of the next section (moved rostrally) was determined on a subject-by-subject basis to overlap, by approximately one vertebral level, the rostral-most position in the previous (caudal) section for which midcoronal spinal cord data were available. Alternatively, if the curvature of the cord was severe, the rostral section was positioned at a level for which midcoronal data could be acquired over a continuous length of cord spanning 15 mm or more (approximately the height of one vertebral body).

Data Analysis

Cardiac-related spinal cord motion was characterized by using methods described previously by Figley and Stroman.[15] For each midline sagittal or coronal dataset, a seed point was manually selected at the spinal cord/CSF interface, typically near the rostral margin of the image acquired at the first cardiac phase (peripheral systole). From this point, an automated algorithm tracked the edge of the cord inferiorly by analyzing voxel-wise signal intensities in a moving grid. This was accomplished by virtue of the stark contrast between spinal cord tissue and CSF and the fact that the signal intensity of each voxel is, therefore, indicative of the cord-to-CSF ratio contained therein. The cord/CSF interface was initially defined along the cord by locating voxels of median signal intensity, and subsequent changes in the cord/CSF ratio throughout the cardiac cycle (ie, cord motion) were quantified by corresponding signal intensity fluctuations. Thus, motion along the spinal cord was quantified with subvoxel precision at 24 phases of the cardiac cycle.

Cord motion in the A/P direction was typically able to be characterized over a large span: most often throughout the entire length of the thoracic and, if need be, the upper-lumbar vertebrae (ie, the upper-thoracic or lower-cervical spinal cord segments to the conus medullaris), depending on subject-to-subject variations in spinal cord length and curvature. Primarily because of the large intersubject differences in A/P spinal cord curvature, L/R cord motion was typically measured (with greater R/C variability) throughout the thoracic and upper-lumbar vertebral levels. For all of the experiments, spinal cord displacement was measured along the cord in 3-mm R/C increments but binned and averaged into 5-mm segments to reduce the number of data points.

As reported previously, segmented CINE acquisitions produce images that are reconstructed over a large number of cardiac cycles, thereby minimizing contributions from swallowing, respiration, and other physiologic or stochastic components that are unrelated to cardiac phase.[15] Furthermore, both intrasubject and intersubject heart rates are automatically normalized, allowing cord motion to be compared, combined, and averaged within and across subjects. Thus, areas of intrasubject overlap (approximately one vertebral level between rostral and caudal FOVs) were averaged according to R/C position, and both A/P and L/R motion data were aligned according to vertebral level before averaging the corresponding R/C levels across subjects.

Results

Cardiac-related thoracic, lumbar, and sacral spinal cord motion was measured in 8 healthy volunteers, and the pattern of oscillatory A/P motion was consistent with previous literature.[15] Maximum cord displacement was observed approximately midway through the cardiac cycle, and the magnitude was found to be dependent on cardiac phase, as well as R/C cord position. The Table lists the maximum A/P and L/R cord displacements (across cardiac phase and R/C position), as well as the corresponding vertebral levels, for each subject. These were typically observed at or near the most rostral level measured and were consistently larger in the A/P (mean ± SD, 0.36 ± 0.13 mm), as opposed to the L/R (mean ± SD, 0.15 ± 0.07 mm) direction. All of the subjects displayed maximum A/P displacement (ie, the largest component) above the T8/T9 intervertebral disk (corresponding roughly with the ninth thoracic spinal cord segment)[9]; and all but 2 of the subjects (ie, 4 and 7, who also happened to be the subjects with the 2 lowest maximum A/P displacements) exhibited maximal displacement at or above the T5 vertebral level (corresponding with the fifth thoracic cord segment).[9]

The maximum values of A/P and L/R cord displacement are shown for every subject

Subject No.	Maximum A/P Displacement, mm	Maximum L/R Displacement, mm
1	0.64 (T3)	0.18 (T7)*
2	0.29 (T2)	0.27 (T3)
3	0.42 (T5)	0.16 (T6)
4	0.20 (T7)	0.12 (T9)
5	0.39 (T2)	0.20 (T4)*
6	0.34 (T3)	0.09 (T3)*
7	0.26 (T8)	0.09 (T9)*
8	0.34 (C3)*	0.09 (T9)*

Note:—A/P indicates anteroposterior; L/R, left-right. Values are listed in millimeters, along with the corresponding vertebral level. Maximum values were often observed at or near the most rostral level measured, and in all of the cases, maximum A/P displacement (mean ± SD, 0.36 ± 0.13 mm) exceeded maximum L/R displacement (mean ± SD, 0.15 ± 0.07 mm).
* Indicates that maximum displacement was observed at the most rostral vertebral level for which data were available in a given subject.

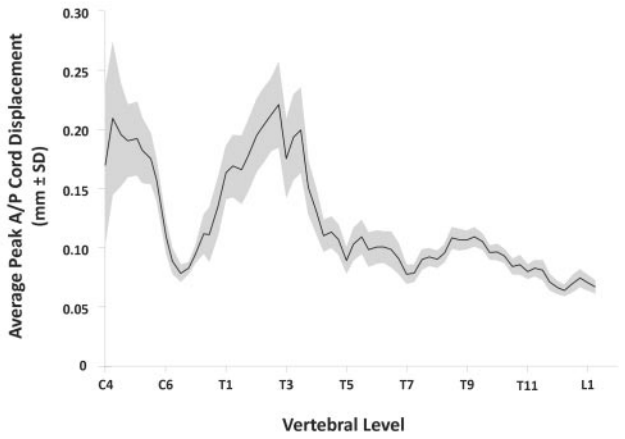

Fig 2. The peak A/P spinal cord displacement averaged across all of the subjects and plotted as a function of R/C cord position (ie, vertebral level). The *black line* indicates the cross-subject average of peak displacement, whereas the *gray area* indicates the region within 1 SD of the mean at each R/C position. Motion below the level of midthoracic vertebrae (around T4 or T5) is significantly lower compared with more rostral cord regions.

Figure 2 shows the peak A/P displacement averaged across all of the subjects and plotted as a function of vertebral level (ie, R/C position along the cord). "Peak" values, at each R/C level, represent the maximum cord displacement in either direction (ie, anterior or posterior) at any cardiac phase. The average was then taken across all of the subjects for whom data were available at a given R/C level. However, because only some subjects' spinal cords move appreciably (and the rest exhibit little or no spinal cord motion), the average was attenuated, and the SD increased at R/C levels where motion was most prevalent (ie, the cervical and upper-thoracic regions).

It is evident, especially for those people whose cords exhibit substantial cardiac-related A/P motion, that the displacements are larger in rostral cord regions (ie, at the level of the cervical and upper-thoracic vertebrae). An example of this is clearly shown by plotting the A/P cord motion of a single subject (subject 1) in Fig 3. In this figure, upper-thoracic cord motion occurs in an oscillatory pattern with a maximal displacement of 0.64 mm midway through the cardiac cycle and at the level of the third thoracic vertebra (T3). In contrast,

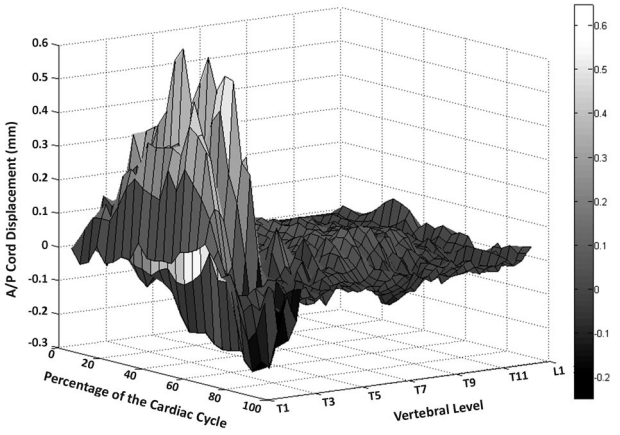

Fig 3. Cardiac-related A/P motion data from a typical subject exhibiting motion of this type. Spinal cord displacement is indicated as a function of cardiac phase and R/C cord position (ie, vertebral level). Positive displacement values indicate anterior motion, whereas negative values indicate posterior motion. Clearly, cord displacements are maximal midway through the cardiac cycle and only at the level of upper-thoracic vertebrae. Conversely, motion dies off and is minimal (at any cardiac phase) at the level of mid- to lower-thoracic vertebrae. This pattern of decreasing motion along the cord, and quiescence in caudal regions, was also evident in other test subjects.

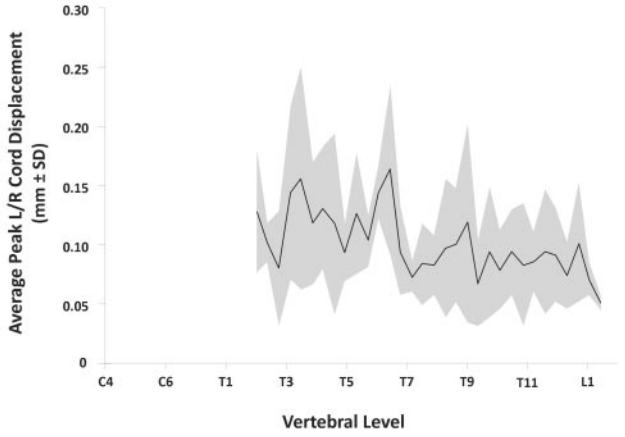

Fig 4. The peak L/R spinal cord displacement averaged across all of the subjects and plotted as a function of R/C cord position (ie, vertebral level). The *black line* indicates the cross-subject average of peak displacement, whereas the *gray area* indicates the region within 1 SD of the mean at each R/C position. To facilitate comparisons between cord motions in each direction (A/P and L/R), the scale has been normalized to that shown for the larger A/P displacements (plotted in Fig 2). Note, however, that the average peak displacement is not significantly larger than 0.10 mm (the estimated measurement precision) at any R/C position, except at the level of T6.

more caudal regions of the spinal cord are relatively motionless, with the motion amplitude decreasing along the cord. As shown in Fig 2, this trend is relatively consistent across our sample population: the average displacement at lower-thoracic vertebral levels is minimal (approximately 0.10 mm), which, along with low SD ($<$0.01 mm), is indicative of uniformly low spinal cord displacements in these regions. Thus, in those subjects exhibiting cardiac-induced A/P spinal cord motion, a consistent pattern arises: significant displacement occurs throughout the cervical and upper-thoracic vertebral levels but is progressively dampened in the caudal direction until, in all of the subjects, it is virtually nonexistent by the lower-thoracic and upper-lumbar vertebral levels (ie, the lower-thoracic, lumbar, and sacral spinal cord regions).

As observed previously at the cervical and upper-thoracic levels,[15] peak L/R spinal cord displacements (throughout the thoracic, lumbar, and sacral levels) were smaller than those measured in the A/P direction. Figure 4 shows the cross-subject average of peak spinal cord displacement as a function of R/C position along the cord. As in Fig 2, these data are collapsed across cardiac phase and represent the peak displacement in terms of the corresponding vertebral level. With the exception of one point (at the level of the T6 vertebra), Fig 4 shows that peak L/R cord displacement is not more than 1 SD above 0.10 mm (the estimated precision of the method) at any R/C position. Moreover, this type of small apparent L/R motion may in fact result as a consequence of the larger A/P motion, because the cord motion through the midcoronal section may slightly alter the observed portion of the cord boundary over the imaging time course.

Discussion

Spinal cord motion has been characterized previously, but not (to the best of our knowledge) in terms of the A/P and L/R motions in lumbar and sacral regions. Although motion in these directions has been thoroughly characterized in cervical and upper-thoracic regions, there is existing literature to suggest that motion may change according to cord position. Feinberg and Mark[19] measured R/C velocities in both the brain stem and lumbar spinal cord, noting that the maximum velocity of the brain stem was greatly pronounced in comparison with the thoracic/lumbar junction of the spinal cord (1.3 $\pm$ 0.44 mm/s versus 0.33 $\pm$ 0.3 mm/s, respectively). A subsequent study by Levy et al[11] reported pulsatile R/C spinal cord velocities up to 12.40 $\pm$ 2.92 mm/s at the cervical and upper-thoracic levels, also noting that cord velocities appeared to decrease caudally along the cord.

The present analysis of A/P and L/R displacement (as a function of R/C cord position and cardiac phase) shows that the spinal cord oscillates in a predictable cardiac-related pattern, consistent with previous investigations of A/P and L/R spinal cord motion.[15] In cervical and upper-thoracic regions, spinal cord displacements have been shown to be larger in the A/P, as opposed to the L/R direction,[15] and the present data demonstrate that this trend continues into lower spinal cord regions as well, with negligible L/R motion observed throughout the lower-thoracic, lumbar, and sacral regions. As expected, A/P cord motion is prevalent throughout rostral (ie, cervical and upper-thoracic) spinal cord segments but is dampened caudally along the cord, with motion in the caudalmost segments falling below the resolution of our technique ($\leq$0.10 mm)[15] for most subjects.

The discovery that lumbar and sacral spinal cord regions are essentially motionless has obvious and important implications for both structural and functional spinal cord imaging; namely, a region free of motion will also be free of motion-related confounds, which are known to be problematic for both spinal fMRI and DTI in cervical regions.[16-18] Because the effects of motion will be significantly reduced, or even absent, in caudal spinal cord regions (compared with cervical regions), the sensitivity and selectivity of spinal fMRI methods can be evaluated under optimal in vivo conditions by using lower-body motor tasks or somatosensory stimulation to examine lumbar and sacral (instead of cervical) spinal cord ac-

tivity. Likewise, DTI in lumbar and sacral spinal cord regions should provide more accurate diffusion tensors than those acquired previously from the cervical cord, yielding better estimates of apparent diffusion coefficients, mean diffusivities, fractional anisotropies, and principal eigenvectors in spinal cord white matter. Thus, by providing an internal criterion standard, the acquisition of uncorrupted data from lumbar regions may present a means of validating compensatory methods.

Conclusions

We found that the magnitude of cardiac-related spinal cord motion varied on a subject-by-subject basis, with some subjects exhibiting little or no motion at all, depending on R/C position. However, even for subjects showing motion throughout the cord, the magnitude of cord displacement was found to be highly dependent on motion direction, cardiac phase, and R/C position along the cord. In the A/P direction, maximal cord displacements consistently occurred midway through each heartbeat, primarily at the level of the cervical and upper-thoracic vertebrae. At the level of the lower-thoracic and upper-lumbar vertebrae (ie, lumbar and sacral cord regions), however, average peak displacement was found to be negligible (routinely <0.10 mm). Similarly, the measurements of L/R motion revealed that cord displacements in this direction are uniformly small throughout the thoracic vertebrae (also, if anything, showing smaller peak values at the lower-thoracic levels). These findings are consistent with previous measurements of R/C motion,[19] suggesting that, overall, the lumbar and sacral spinal cord segments are essentially motionless in all 3 of the spatial dimensions. Because spinal cord motion is known to be a confounding factor for both spinal DTI and fMRI, the discovery that this region of the cord is motionless has significant implications for both structural and functional spinal cord imaging.

Acknowledgments

We thank Sharon David for technical assistance, Teresa McAdam for helping with figure preparation, and the other members of the Stroman Lab (Niousha Foad Ghazni, Celina Nahanni, Natalie Kozyrev, and Randi Beazer) for reviewing the manuscript.

References

1. Stroman PW, Tomanek B, Krause V, et al. **Mapping of neuronal function in the healthy and injured human spinal cord with spinal fMRI.** *NeuroImage* 2002;17:1854–60
2. Wilmink JT, Backes WH, Mess WH. **Functional MRI of the spinal cord: will it solve the puzzle of pain?** *JBR-BTR* 2003;86:293–94
3. Stroman PW, Kornelsen J, Bergman A, et al. **Non-invasive assessment of the injured human spinal cord by means of functional magnetic resonance imaging.** *Spinal Cord* 2004;42:59–66
4. Stroman PW. **Magnetic resonance imaging of neuronal function in the spinal cord: spinal FMRI.** *Clin Med Res* 2005;3:146–56
5. Kornelsen J, Mackey S. **Potential clinical applications for spinal functional MRI.** *Curr Pain Headache Rep* 2007;11:165–70
6. Clark CA, Werring DJ. **Diffusion tensor imaging in spinal cord: methods and applications—a review.** *NMR Biomed* 2002;15:578–86
7. Ozanne A, Krings T, Facon D, et al. **MR diffusion tensor imaging and fiber tracking in spinal cord arteriovenous malformations: a preliminary study.** *AJNR Am J Neuroradiol* 2007;28:1271–79
8. Vargas MI, Delavelle J, Jlassi H, et al. **Clinical applications of diffusion tensor tractography of the spinal cord.** *Neuroradiology* 2008;50:25–29
9. Blumenfeld H. *Neuroanatomy Through Clinical Cases.* Sunderland, Mass: Sinauer Associates, Inc; 2002:22–24
10. Jokich PM, Rubin JM, Dohrmann GJ. **Intraoperative ultrasonic evaluation of spinal cord motion.** *J Neurosurg* 1984;60:707–11
11. Levy LM, Di CG, McCullough DC, et al. **Fixed spinal cord: diagnosis with MR imaging.** *Radiology* 1988;169:773–78
12. Enzmann DR, Pelc NJ. **Brain motion: measurement with phase-contrast MR imaging.** *Radiology* 1992;185:653–60
13. Mikulis DJ, Wood ML, Zerdoner OA, et al. **Oscillatory motion of the normal cervical spinal cord.** *Radiology* 1994;192:117–21
14. Kohgo H, Isoda H, Takeda H, et al. **Visualization of spinal cord motion associated with the cardiac pulse by tagged magnetic resonance imaging with particle image velocimetry software.** *J Comput Assist Tomogr* 2006;30:111–15
15. Figley CR, Stroman PW. **Investigation of human cervical and upper thoracic spinal cord motion: implications for imaging spinal cord structure and function.** *Magn Reson Med* 2007;58:185–89
16. Figley CR, Stroman PW. **A new method of motion-compensated spinal fMRI: identifying human spinal cord function with increased sensitivity and reproducibility.** *Proceedings of the International Society for Magnetic Resonance in Medicine 15th Annual Meeting*, May 19–25, 2007; Berlin, Germany
17. Kharbanda HS, Alsop DC, Anderson AW, et al. **Effects of cord motion on diffusion imaging of the spinal cord.** *Magn Reson Med* 2006;56:334–39
18. Summers P, Staempfli P, Jaermann T, et al. **A preliminary study of the effects of trigger timing on diffusion tensor imaging of the human spinal cord.** *AJNR Am J Neuroradiol* 2006;27:1952–61
19. Feinberg DA, Mark AS. **Human brain motion and cerebrospinal fluid circulation demonstrated with MR velocity imaging.** *Radiology* 1987;163:793–99